SPECTRAL CHARACTERISTICS OF THE 1960 TSUNAMI AT CRESCENT CITY, CA

Linda Holmes-Dean
Scientific Marine Services Inc
955 Borra Place, Suite 100, Escondido, CA 92029, USA
ldean@scimar.com

Myrl Hendershott
Scripps Institution of Oceanography, UCSD, La Jolla, CA 92093, USA

Peter D. Bromirski
Scripps Institution of Oceanography, UCSD, La Jolla, CA 92093, USA

Reinhard E. Flick
California Department of Parks and Recreation
Division of Boating and Waterways, Scripps Institution of Oceanography, UCSD, La Jolla, CA 92093, USA

ABSTRACT

Spectral characteristics of sea level fluctuations during the May 1960 Chilean Earthquake tsunami are investigated using digitized strip chart recordings from two docks within Crescent City Harbor. Peaks in sea level spectra at the two docks near 10^{-3} Hz and near 2.1×10^{-3} Hz correspond to the two lowest frequency harbor modes, occurring above the frequency band most strongly excited by the tsunami. Tidal modulation of harbor spectral structure at very short periods is observed. Theoretical estimates of shelf edge wave resonant modes fall within the frequency band strongly excited by the tsunami, in contrast to modeled edge waves from a seismic event near Cape Mendocino that show no evidence of the reflection necessary for a strong shelf resonance. This suggests that heightened susceptibility of sea level (but not necessarily currents) at Crescent City to tsunami is not due primarily to either harbor or shelf resonances.

Keywords: Crescent City Harbor, tsunami tidal modulation, marigram digitization, harbor modes

1. INTRODUCTION

Crescent City, located on the California coast about 460 km north of San Francisco, has suffered greater damage from tsunamis in historic times than any other community on the West Coast of the North America [*Dengler and Magoon* 2006]. Previous studies of individual tsunami events at Crescent City have invoked the importance of source directionality [*Wiegel* 1976; *Hatori* 1993], focusing of wave energy by offshore bathymetry [*Roberts and Chien* 1964], and resonant shelf oscillations [*Wilson and Torum* 1968; *Gonzalez et al.* 1995] to explain high tsunami amplitudes at Crescent City.

The two possible explanations for local amplification considered in this paper are (1) near-resonant oscillations in the Crescent City harbor, and (2) near-resonant oscillations on the shelf adjacent to Crescent City [*Horillo et al.* 2008].

A record of the observations of the 1960 Chilean tsunami at Crescent City was provided by virtually continuous strip chart recordings over 11 May 1960 to 16 June 1960 from pressure gauges in stilling wells at two locations in the harbor [*Kendall et al.* 2008]. *Magoon* [1962] digitized and analyzed a small portion of this record. *Holmes-Dean et al.* [2009] digitized an eleven-day interval 20 May 1960 to 31 May 1960 that captures both the onset and decay at a sampling frequency of one Hz. The data and digitization procedures are documented in *Holmes-Dean et al.* [2009].

The present day harbor configuration and the 1960 locations of the two pressure gauges, at Dutton's Dock and at Citizen's Dock (the present day NOAA tide gauge is very near Citizen's dock), are shown in Figure 1a. The geometry of the harbor was modified in 1972 by carving the 200 x 300 m Small Boat Basin into the northeastern shore of the harbor, northward of Citizen's dock [*Dengler and Uslu* 2011]

2. THE TSUNAMI IN THE TIME DOMAIN

The digitized records of sea level at the two pressure gauges as well as the NOAA predicted tide for Crescent City are displayed in Figure 1b. The records span from two days after the beginning of digitization, encompassing several hours after the onset of the tsunami arrivals at about 0220 PST, 23 May 1960 [*Magoon* 1962].

The two records are not identical. They differ not only at short time scales, but also because of apparent timing errors in either or both of the two records. In some instances, timing error is clearly associated with a shift from one strip chart record to the next (each strip chart record spans about 24 hours). In other instances, the error appears to vary slowly over many hours. The origins of these errors are fully discussed in *Holmes-Dean et al.* [2009]. An attempt to further reduce this error is discussed below.

3. SEA LEVEL SPECTRA

All spectra, S(f), discussed below are estimates of one-sided power spectra with signal variance given by $\int_0^\infty S(f)\, df$.

Individual spectra for each of the seven days following the onset of the tsunami are shown at Citizen's dock in Figure 2a and at Dutton's dock in Figure 2b. Also shown are pre-tsunami and post-tsunami spectra (plotted two decades lower than the seven day spectra for easy distinction). Estimates of the frequency and period corresponding to each of the features labeled in Figure 2 are given in Table 1. In subsequent discussion, these features are referenced using the identifying labels given in Table 1.

(Robert Campbell photograph)
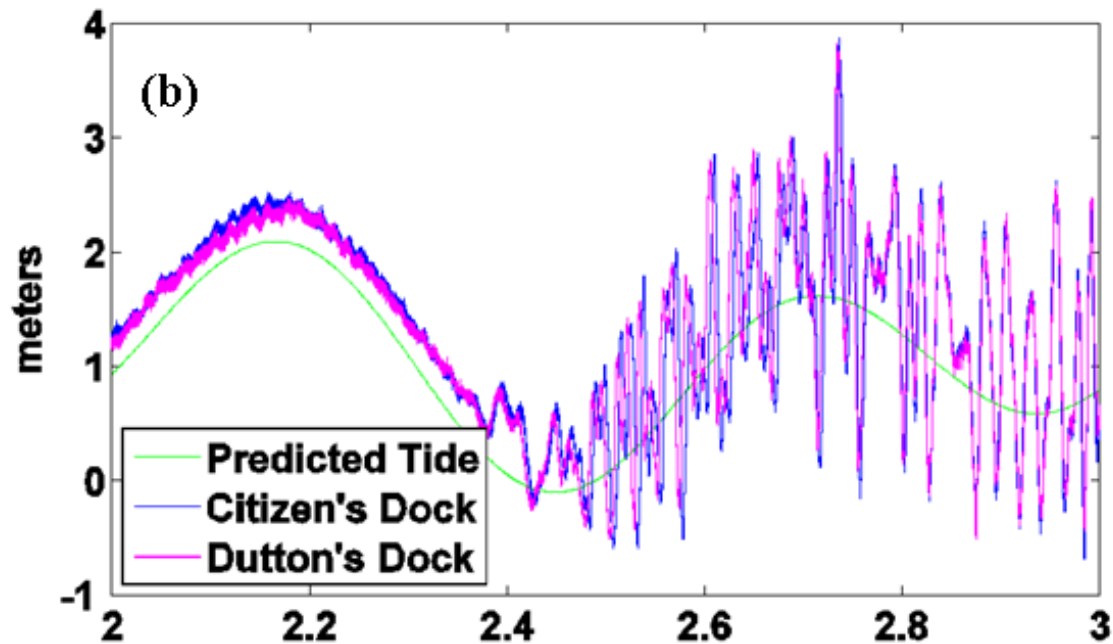
Figure 1. (a) Crescent City Harbor with locations of pressure gauges at Dutton's dock (northwestern corner of the harbor) and at Citizen's dock to the east behind the eastern inner harbor jetty, with the current NOAA Crescent City tsunami tide gauge location (yellow star). Note that the Small Boat Basin in the northeastern corner of the harbor was built in 1972 (*Dengler et al.*, 2011). Dutton's Dock has been replaced and realigned since the 1960 Chilean tsunami sea level data were recorded. (b) Predicted tide (green line) and sea level at Dutton's dock and at Citizen's dock as determined hydrostatically from pressure gauge records over a one-day interval spanning the onset of the tsunami arrivals from the Chilean earthquake of May 1960.

The spectra at the two gauges are nearly equal to one another day by day at frequencies below the break frequency, $f_{br} \sim 10^{-3}$ Hz, at which they clearly diverge. At frequencies lower than the break frequency, the pre-tsunami and post-tsunami spectra fall off less steeply than the f^{-2} falloff for open ocean background spectra found by *Filloux et al.* [1991] and *Rabinovich et al.* [2011]. At frequencies immediately above f_{br}, all the spectra begin to decrease significantly more rapidly than the f^{-2} background falloff.

At both docks the spectra become indistinguishable from the pre-tsunami and post-tsunami background at and above a high frequency, f_{hi}, at about 7×10^{-3} Hz. At Citizen's dock (in the eastern part of the harbor), the fall off from f_{br} is interrupted by sharp spectral peaks (identifiable in each daily spectrum) at $f_{cd1} \sim 2.1 \times 10^{-3}$ Hz, $f_{ci2} \sim 8 \times 10^{-3}$ Hz, and $f_{ci3} \sim 1.8 \times 10^{-2}$ Hz. At Dutton's dock (in the western harbor, directly exposed to the harbor mouth), the fall off from f_{br} is interrupted by the sharp peak at $f_{cd1} \sim 2.1 \times 10^{-3}$ Hz, also visible at Citizen's dock, and by very broad peaks that have no counterparts at Citizen's dock centered near $f_{du2} \sim 5 \times 10^{-3}$ Hz and $f_{du3} \sim 2 \times 10^{-2}$ Hz.

Table 1. Spectral features labeled in Figure 2

Frequency Label	Description	Frequency (Hz)	Period
f_{lo}	rough lower limit of the frequency range excited by the tsunami	$\sim 10^{-4}$	~ 2.8 hours
f_{hi}	rough upper limit of the frequency range excited by the tsunami; frequency at which the spectrum on the first day of the tsunami drops below spectra on subsequent days	$\sim 7 \times 10^{-3}$	~ 2.4 min
f_{br}	frequency at which spectra at both gauges suddenly break from being nearly flat to rapidly falling off	$\sim 10^{-3}$	~ 16.7 min
f_{cd1}	central frequency of lowest frequency sharp peak on all spectra at both gauges	$\sim 2.1 \times 10^{-3}$	~ 7.9 min
f_{ci2}	central frequency of second peak on all Citizen's dock spectra	$\sim 8 \times 10^{-3}$	~ 2.1 min
f_{ci3}	central frequency of third peak on all Citizen's dock spectra	$\sim 1.8 \times 10^{-2}$	~ 56 s
f_{du2}	central frequency of second (very broad) peak on all Dutton's dock spectra	$\sim 5 \times 10^{-3}$	~ 3.3 min
f_{du3}	central frequency of second (very broad) peak on all Dutton's dock spectra	$\sim 2 \times 10^{-2}$	~ 50 s

The range of frequencies clearly excited during the tsunami begins slightly below $f_{lo} \sim 10^{-4}$ Hz (Figure 2). The spectrum on the first day of the tsunami is indistinguishable from that of the next day for frequencies higher than roughly $f_{hi} \sim 7 \times 10^{-3}$ Hz. At first glance it appears that the spectral levels during the tsunami's final day (solid black line) lie below that of the previous days at frequencies as high as 6×10^{-2} Hz (~ 17 s), so that sea level variance up to this frequency might be thought to be associated with tsunami arrivals. But this at least in part reflects the fact that sea level variance at these frequencies is also associated with background processes not related to the tsunami whose intensity varies day by day. Thus, for example, the *least* energetic of all the spectra in Figures 2a and 2b is the spectrum for the seventh day of the tsunami and not, as might have been thought, the post-tsunami spectrum.
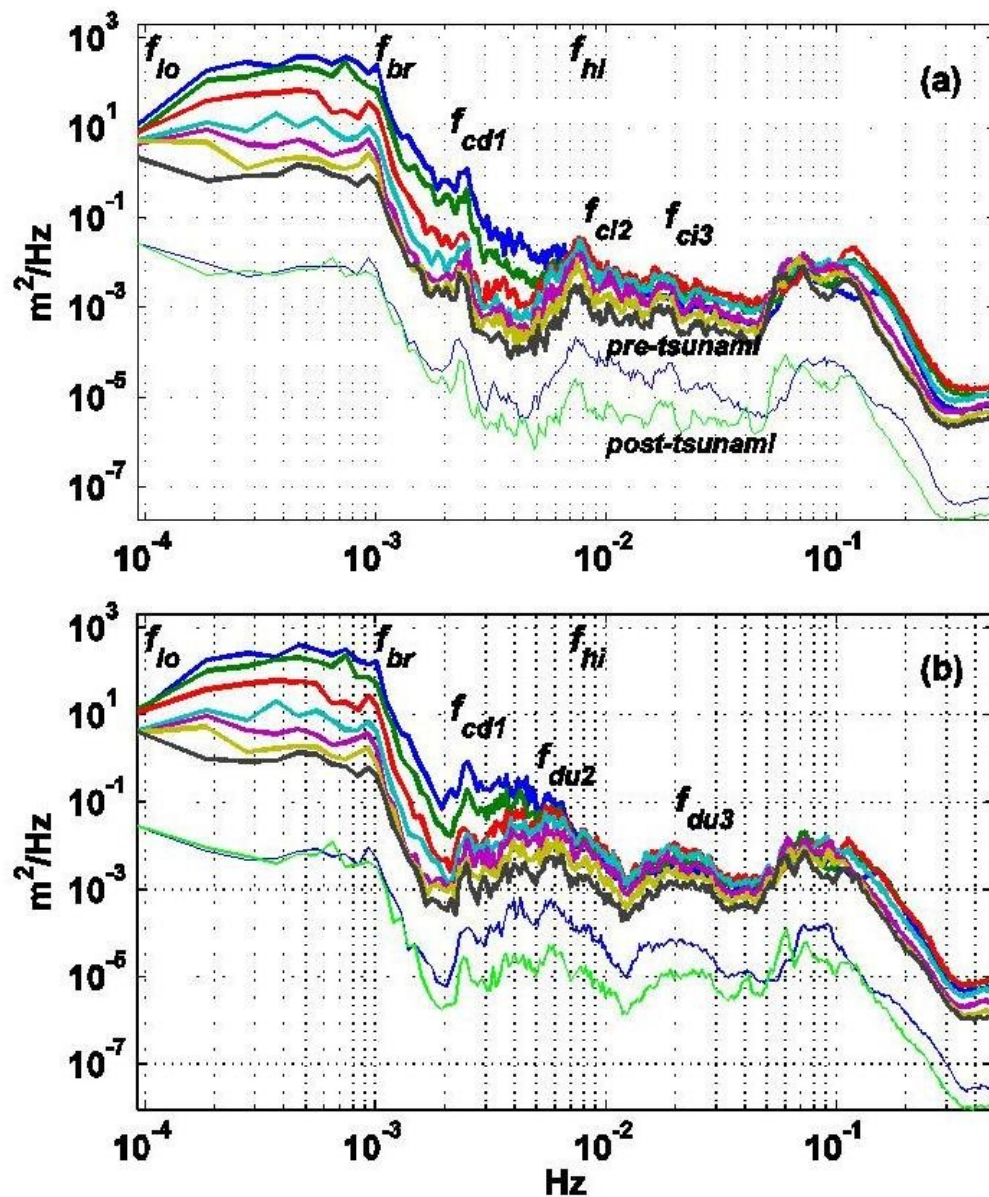
Figure 2. (a) At Citizen's dock: Upper seven curves are sea level spectra (m^2/Hz) for the first seven days of tsunami arrivals (over the lowest decade in frequency, the spectrum for each day is above that for all following days), pre- and post-tsunami spectra (thin blue and green lines, respectively) are displaced downward vertically by two decades for ready visualization. Each spectrum is calculated from two days of de-tided record broken into 50% overlapping Hamming-windowed six-hour segments. Note that (i) the post-tsunami spectrum (thin green line) has *lower* spectral levels than the pre-tsunami spectrum (thin blue line) for frequencies above 10^{-3} Hz, and (ii) the first day tsunami spectral levels (uppermost curve) drop below those for subsequent days at about 7×10^{-3} Hz (f_{hi}). Labels f_{lo}, f_{br}, apply to specific spectral peaks and characteristics discussed in the text. (b) Same as (a) but for Dutton's dock.

Within the frequency range clearly attributable directly to the tsunami between $f_{lo} \sim 10^{-4}$ Hz and about $f_{hi} \sim 7 \times 10^{-3}$ Hz (Figure 2), the spectra decay monotonically in time at each frequency. However, as shown in Figure 2, for frequencies above about 2×10^{-3} Hz, sea level variance associated with background processes unrelated to the tsunami (e.g. the pre- and post-tsunami spectra) is comparable to tsunami induced changes in spectral levels at the high end of the range of frequencies excited by the tsunami. Thus it is not possible to ascertain whether tsunami spectra at higher frequencies decay in time appreciably faster than tsunami spectra at lower frequencies.

4. HARBOR AND SHELF RESONANCES

Below we compare various of the observed spectral peaks noted above with numerical estimates of resonance frequencies within Crescent City harbor and over the continental shelf adjacent to Crescent City from previous studies.

4.1 Numerically estimated harbor resonances

Horillo et al. [2008] solve a shallow water model of Crescent City harbor sea level variation for the first four (longest period) harbor normal modes with mean depths differing by two meters, corresponding to high tide (MHHW) and low tide (MLLW), obtaining the periods and corresponding natural frequencies given in Table 2. Model sea level has a node at the open mouth of the harbor. From low tide to high tide, the first and second numerical mode frequencies shift towards higher frequencies, in qualitative agreement with what one expects for modes whose natural frequency depends on the shallow water wave speed. But remarkably the reverse occurs for the third and fourth numerical modes; from low tide to high tide their frequencies shift towards lower frequencies. Some evidence of the former behavior is described in the following analysis of the records, but not of the latter.

Table 2. Harbor Mode Numerical Model Results of *Horillo et al.* [2008]

Frequency Label	Description	Period	Frequency (Hz)
Harbor normal modes at high tide			
$f^{MHHW}(1)$	Mode 1 High Tide	14.45 min	1.15×10^{-3}
$f^{MHHW}(2)$	Mode 2 High Tide	7.68 min	2.17×10^{-3}
$f^{MHHW}(3)$	Mode 3 High Tide	7.28 min	2.29×10^{-3}
$f^{MHHW}(4)$	Mode 4 High Tide	5.68 min	2.93×10^{-3}
Harbor normal modes at low tide			
$f^{MLLW}(1)$	Mode 1 Low Tide	15.68 min	1.06×10^{-3}
$f^{MLLW}(2)$	Mode 2 Low Tide	9.01 min	1.85×10^{-3}
$f^{MLLW}(3)$	Mode 3 Low Tide	6.38 min	2.61×10^{-3}
$f^{MLLW}(4)$	Mode 4 Low Tide	4.71 min	3.54×10^{-3}

Agreement between these model normal mode frequencies and those of our spectral peaks has to be limited at least because (i) the open mouth condition imposed in the model is not exact, and (ii) the shape of the harbor modeled is different from the harbor shape during the 1960 tsunami. The tidal modulation of the spectra shown in Figure 2 is investigated below.

(i) In the shallow water model of *Horillo et al.* [2008], sea level is forced to have a node at the mouth of the harbor. If the true harbor modes are radiatively coupled to external shelf modes or to the open ocean, these estimates of harbor normal mode frequencies are, by analogy with Rayleigh's correction for an open-ended organ pipe [*Rayleigh* 1904], likely to be somewhat high. The general problem of coupling harbor oscillations to a larger exterior domain has been discussed by *Miles* [1974]. Simple application of his methods to the Crescent City region is beyond the scope of this paper because the exterior domain begins with offshore deepening continental-shelf bottom relief that can potentially support edge waves, well outside Crescent City Harbor.

(ii) The Small Boat Basin shown on Figure 1a was carved into the northeast shore of the harbor in 1972 [*Dengler and Uslu* 2011]. This harbor modification significantly affects any comparison of features of the 1960 spectra with the model results of *Horillo et al.* [2008] because the model sea level variance associated with the second and third modes of *Horillo et al.* [2008, their figure 4] is strongly concentrated in the Small Boat Basin just north of Citizen's dock (Figure 1a) at low tide, (although not at high tide). These model modes may thus not closely resemble the modes of the harbor at the time of the 1960 tsunami.

4.2 Evidence for tidal modulation

Tidal modulation of the period of a harbor seiche at Grindavik Harbor, Iceland, has been reported by *Donn and Wolf* [1972], and *Lee et al. [2012]* have emphasized the importance of allowing for tidal variation in interpreting spectra of sea level variance associated with tsunami. Accordingly, spectra of sea level at Citizen's dock and Dutton's dock were constructed as averages over three-hour intervals centered first at high tide and then at low tide (Figure 3). The spectral peaks at Citizen's dock (f_{cd1}, f_{ci2}, f_{ci3}) and at Dutton's dock (f_{cd1}, f_{du2}, f_{du3}) identified in Figure 2 can be identified in Figure 3, but are not as well resolved as in Figure 2 because of the shorter record length necessitated by analyzing high and low tide segments. The shifts of the first two model normal mode frequencies towards higher frequency from low to high tide is a consequence of increasing gravity wave phase speed with increased water depth, i.e. $f^{MLLW}(1) \sim 1.06 \times 10^{-3}$ Hz to $f^{MHHW}(1) \sim 1.15 \times 10^{-3}$ Hz and $f^{MLLW}(2) \sim 1.85 \times 10^{-3}$ Hz to $f^{MHHW}(2) \sim 2.17 \times 10^{-3}$ Hz, which can correspondingly not be resolved.

Yet the entire spectrum at Dutton's dock (Figure 3b), over the frequency band from roughly 6×10^{-3} Hz (~ 2.8 min) to about 3×10^{-2} Hz (~ 33 s), shifts towards higher frequencies from low tide to high tide with little change in shape. In particular, at Dutton's dock (but not Citizen's), the broad peak labeled f_{du2} shifts about 0.1×10^{-2} Hz towards higher frequency from low to high tide. The lower limit of this range over which the shift can be identified is not well defined, in part because of the shortness of the segments necessitated by stratification of observations between high and low tide. In contrast at Citizen's dock (Figure 3a), there is little if any systematic difference between the spectra at high and low tide.
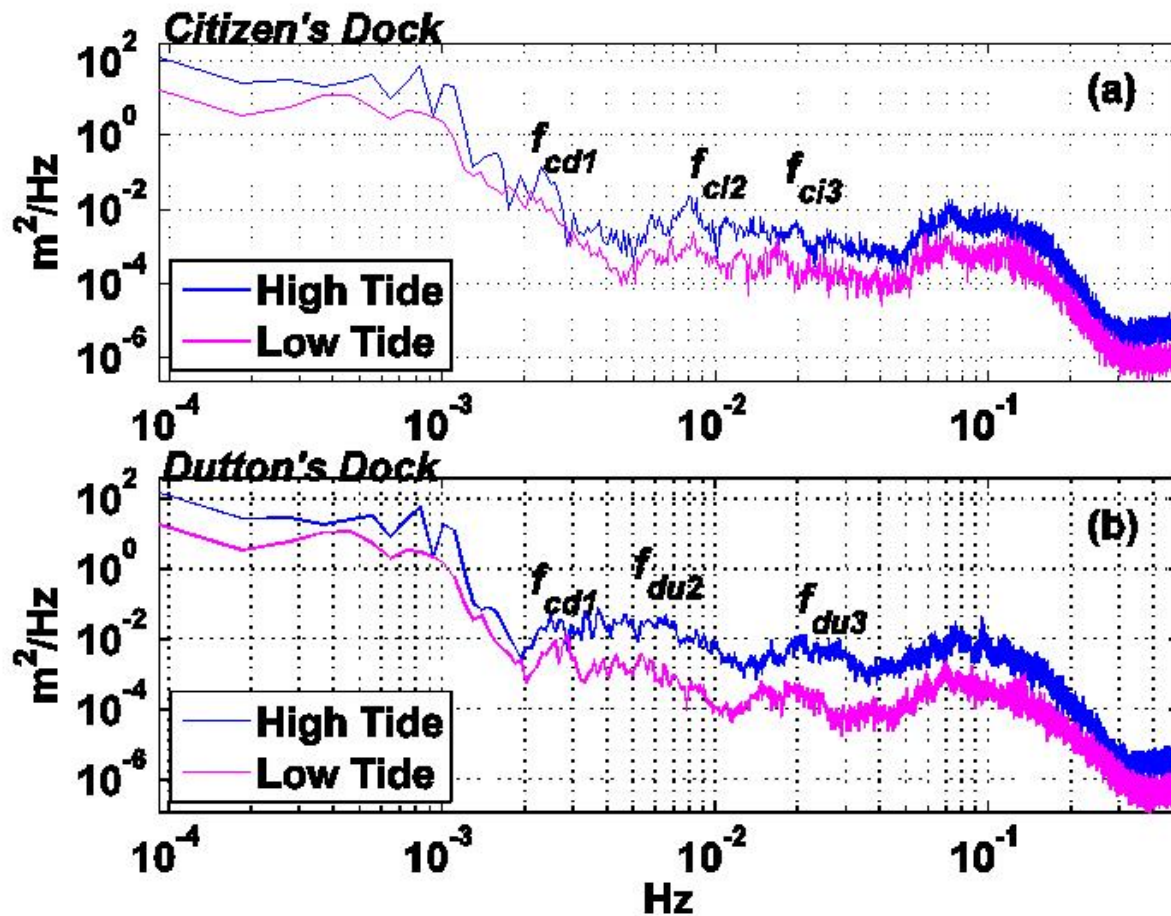
Figure 3. (a) Sea level spectra (m^2/Hz) at Citizen's dock estimated from three-hour segments of de-tided sea level fluctuations centered at high tide and low tide. (b) Sea level spectra (m^2/Hz) at Dutton's dock estimated from three-hour segments of de-tided sea level fluctuations centered at high tide and low tide.

The shift of spectral features towards higher frequencies at high tide (Figure 3b), is in accord with that of the first and second modes of *Horillo et al.* [2008; Table 2] at Dutton's dock (in the western part of the harbor, Figure 1). However, no such systematic spectral shift is seen at Citizen's dock (Figure 3a). We have no certain explanation for this observation. One explanation might be that higher frequency modes are trapped against the western wall of the harbor in a manner analogous to that in which one of the modes in Kahului Harbor, (Maui, Hawaii) found by *Okihiro et al.* [1994, their figures 7, 8, 9] is trapped against one wall of the harbor. This speculation is not in very good accord with the spatial structure of the higher modes displayed by *Horillo et al.* [2008], but, as noted above, they may not be representative of the harbor modes at the time of the 1960 tsunami on account of the subsequent construction of the small boat basin.

4.3 Comparison of sea level spectral features with numerically estimated harbor resonances

Prominent peaks are clearly visible in the spectra at both docks, with higher frequency peaks also showing some correspondence (Figure 2). These peaks are associated with harbor modes that characterize water level variability within Crescent City Harbor.

First Mode. The break in spectral levels (f_{br}, Figure 2) appears to correspond to the first (lowest frequency) of the numerically determined harbor modes of _Horillo et al._ [2008; our Table 2]: $f^{MLLW}(1)$ ~ 1.06 x10^{-3} Hz, $f^{MHHW}(1)$ ~ 1.15 x10^{-3} Hz, f_{br} ~ 10^{-3} Hz.

Sea level fluctuations near f_{br} are expected to be well correlated between the two stations, with very similar amplitude and zero phase shift (Figure 4). This is in accord with the first mode in the model simulation of _Horillo et al._ [2008] extending across the entire harbor with little change in shape between high and low tide, and having no interior nodal line. The correlation estimation procedure is discussed below, in Section 4.4.

Second Mode. The next lowest frequency feature of the 1960 tsunami spectra (Figure 2, labeled f_{cd1}), appears to correspond to the second (next lowest frequency) of the numerically determined harbor modes of _Horillo et al._ [2008; our Table 2]: $f^{MLLW}(2)$ ~ 1.85 x10^{-3} Hz, $f^{MHHW}(2)$ ~ 2.17 x10^{-3} Hz, f_{cd1} ~ 2.1 x10^{-3} Hz.

Sea level fluctuations near f_{cd1} are detectably correlated between the two stations (Figure 4), in qualitative accord with the fact that the second mode in the model simulation of _Horillo et al._ [2008] extends across the entire harbor. However, the phase lag is about two radians and not zero or π radians as would be expected for the position of the interior node in the second standing modes of _Horillo et al._ [2008] at low and high tide, respectively.

Higher modes. Sharp higher frequency peaks appear in the Citizen's spectra (at f_{ci2} ~ 8 x10^{-3} Hz and f_{ci3} ~ 1.8 x10^{-2}) Hz, with broad higher frequency peaks also appearing in the Dutton's spectra (centered at f_{du2} ~ 5 x10^{-3} Hz and f_{du3} ~ 2 x10^{-2} Hz). Their frequencies are all somewhat higher than those of the third and fourth modes of _Horillo et al._ [2008; our Table 2]. The two records are not detectably correlated at these frequency peaks (Figure 4), indicating no correspondence with any harbor-wide mode. This lack of correlation may however result from timing errors not being fully removed by the timing-adjustment procedure given in Section 4.4.

The observational picture regarding higher modes is thus incomplete. Since the higher mode frequencies lie above the frequency range within which sea level variation within the harbor is excited by the tsunami, this may have little practical significance for the response of sea level within the harbor to tsunami. However, the same may not be true for the response of currents within the harbor to tsunami.
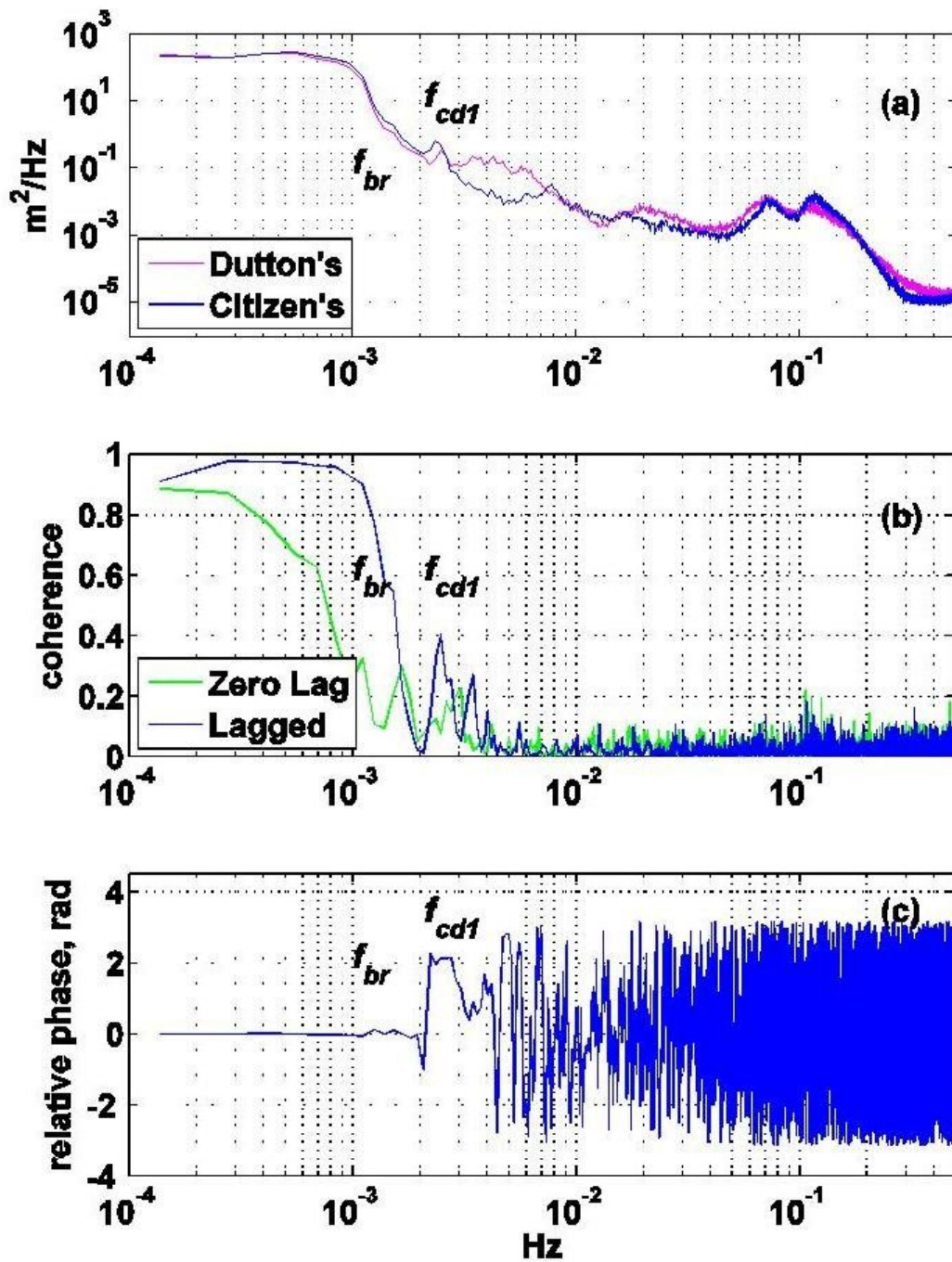
Figure 4. (a) Sea level spectra (m^2/Hz) at Dutton's and Citizen's docks for first three days of tsunami arrivals. Three days are divided into 36 two-hour 50% overlapping Hamming-windowed segments. (b) Coherence between records at Citizen's and Dutton's docks lagged as explained in Section 4.4 (blue line); coherence between the records at Citizen's and Dutton's docks without lag (green line). (c) Relative phase between records at Citizen's and Dutton's docks lagged as explained in Section 4.4.

4.4 Estimation of Correlation within Crescent City Harbor

In order to estimate frequency domain correlations between the two records, the first three days of each de-tided record after the onset of the tsunami (a time when modes are expected to be most strongly energized) were divided into two-hour segments. The frequency correlation (coherence) between Dutton's and Citizens' docks was computed for each segment and then averaged over all segments (Figure 4b). The coherence decreased from near unity to small values over the band spanning 1.4×10^{-4} Hz (~ 2 hours) to about 10^{-3} Hz (~ 16.7 min), with low coherence at higher frequencies but with very small phase shifts over the entire band. If we assume that at least some of the loss of coherence at higher frequencies results from the timing errors noted above, then a possible remedy is to suppose, on physical grounds, that the lowest resolved frequencies are in fact in phase at the two gauges.

Accordingly, the Dutton's and Citizen's records were band passed so that only the variance at periods between 30 min and 90 min was retained. For each sampling instant, the immediately following two hour segment of the band-passed record at Dutton's dock was shifted relative to the corresponding segment of the band passed record at Citizen's dock by a lag chosen to maximize their time domain correlation. The correlations between corresponding segments of the records before band passing were then recomputed at that lag. The resulting correlation and relative phase are shown in Figure 4.

This procedure has forced nearly unit correlation with zero phase lag at frequencies spanning the band from the lowest resolved frequency 1.4×10^{-4} Hz (~ 2 h) to $f_{br} \sim 10^{-3}$ Hz (~ 16.7 min). It additionally allows resolution of a sharp peak in coherence (about 0.4) at about 2.1×10^{-3} Hz, with a nearly constant phase lag. This is the frequency f_{cd1} at which background and tsunami spectra (Figure 2) consistently show a sharp peak. We have thus achieved a modestly enhanced coherence estimate at a frequency that may correspond to that of the second harbor mode of *Horillo et al*. [2008].

4.5 Shelf resonances and edge waves

The modeled harbor modes of *Horillo et al.* [2008] are the most complete in the literature. We have above identified the first two of these modes with features in the sea level spectra. But the spectral region most strongly energized by the tsunami lies at lower frequencies (Figure 2). The pre-tsunami and post-tsunami spectra in this region fall off less steeply than the f^2 falloff for open ocean background spectra found by *Filloux et al.* [1991] and *Rabinovich et al.* [2011]. What then determines the spectral shape in this region? Shelf modes (edge waves) standing or propagating along the coast are an obvious possibility.

Horillo et al. [2008] estimated the spatial patterns and periods of standing shallow water normal modes in a domain exterior to the harbor that spans the coast and the shelf between Pt. St. Georges (a few tens of km north of Crescent City along the coast) and Patrick's Point (some 80 km south of Crescent City along the coast). They imposed boundary conditions of no normal flow at the coast and of no sea level variation (a node) at the offshore 200 m isobath, with straight reflecting boundaries

extending westward from the coast at Pt. St. Georges and Patrick's Point until the offshore 200 m isobath. These boundary conditions allow no flow of energy out of the domain, and thus make possible resonant modes. *Horillo et al.* [2008] find alongshore standing-wave periods within this domain spanning 67 min (2.5 x10^{-4} Hz) to 18 min (9.3 x10^{-4} Hz). (Higher frequency numerical modes no doubt exist but are not reported). Alongshore standing wave modes 1, 4, 6, 7, 8 and 14 are qualitatively similar to alongshore standing-edge waves having mode zero cross-shore structure (monotonic decay away from a maximum at the coast). Other modes displayed have one or two zero crossings offshore.

A number of these shelf modes have natural frequencies in the frequency range $f_{lo} \sim 10^{-4}$ Hz to about $f_{hi} \sim 7$ x10^{-3} Hz most strongly excited by the tsunami, if they were strongly resonant they could contribute appreciably to sea level response to tsunami within Crescent City Harbor.

For standing edge-mode shelf resonances corresponding to the shelf modes of *Horillo et al.* [2008] to occur, there should be strong reflection of coastally-trapped edge waves at coastal features such as Patrick's Point (about 80 km south of Crescent City) and Pt. St. Georges (about 10 km north of Crescent City). Somewhat surprisingly, such reflection does *not* occur in the shallow water model of *Gonzalez et al.* [1995], who modeled disturbances associated with the seismic event of April, 1992 centered near the coast close to Cape Mendocino (about 150 km south of Crescent City). Their model domain spanned the continental shelf, extending from south of Port San Luis (about 800 km south of Crescent City) to north of Point Orford (about 100 km north of Crescent City). The modeled seismogenic coastal edge waves propagated along the coast past Patrick's Point, Crescent City and Pt. St. Georges without any appreciable amplification or reflection. The modeled sea level fluctuations at North Spit (the tide gauge closest to, and north of the epicenter) were about the same amplitude as those observed at the North Spit tide gauge, but modeled sea level fluctuations at the alongshore location near Crescent City were not enhanced relative to those modeled at Crescent City Harbor, and were only about half those observed at the Crescent City Harbor tide gauge (*Gonzalez et al.* 1995, their figure 4).

The model results of *Gonzalez et al.* [1995] thus argue *against* the importance of resonant standing edge mode shelf contributions to the sea level fluctuations observed at Crescent City harbor during the 1960 tsunami. Yet *Horillo et al.* [2008] also find broad peaks corresponding to some (but not all) of these shelf modes in a nonlinear and highly dissipative shallow water model occupying a somewhat larger region, with harmonic forcing at the western boundary and energetics such that the energy influx through the western boundary is balanced by dissipation and energy outflow through the northern and southern boundaries. In particular (their figure 10), they identify a peak in their forced model response at 21 min period (7.9 x10^{-4} Hz), with a peak at the same period in their estimate of the spectrum of de-tided sea level variation at the Crescent City tide gauge associated with the Kuril Island tsunami of 2006. Our spectra are not directly comparable with their spectrum because we have averaged more heavily in order to increase statistical reliability, but the important point is that the *broad* peaks at 21 min (7.9 x10^{-4} Hz), 36 min (4.6 x10^{-4} Hz), 40 min (4.1 x10^{-4} Hz) and 52 min (3.2 x10^{-4} Hz) in their forced model response span much of the spectral region most strongly energized by the 1960 tsunami (Figure 2), an observation in support of harbor response due to adjacent shelf bathymetry for these frequencies.

Further elucidation of the role of shelf edge-wave resonances in the response of Crescent City harbor to tsunami would require either additional measurements on the shelf as well as within the harbor, and/or much more detailed numerical modeling, both beyond the scope of this paper. These results indicate that the simple resonance of either harbor or adjacent shelf modes will not entirely explain the enhanced response of sea level in Crescent City harbor to tsunami. We note however, with *Dengler and Uslu* [2011], that the higher modes may be much more important for the response of currents in the harbor to tsunami than they are for the response of sea level. Further modeling work is needed to resolve this and other questions.

5. SUMMARY

Analog sea level data recorded at two pressure gauges in the harbor at Crescent City in northern California during the tsunami generated by the May 1960 Chilean earthquake have been digitized at a sampling interval of 1 Hz. The records from 20 May 1960 to 31 May 1960 were analyzed to describe sea level variation associated with that tsunami in Crescent City harbor.

Evidence is found for the excitation of harbor modes resembling the two lowest frequency modeled shallow-water harbor modes of *Horillo et al.* [2008]: an abrupt downward trend in spectral slope at both gauges starting very near the frequency of the grave mode ($\sim 10^{-3}$ Hz), and a distinct peak at both gauges near the frequency of the second mode ($\sim 2.1 \times 10^{-3}$ Hz). Coherence between the two gauges at and below the frequency of the grave mode is high and, after removal of timing errors between the two gauges, is detectable at the frequency of the second mode. These harbor resonant frequencies do not however span the lower decade of the frequency band most strongly excited by the tsunami, $\sim 10^{-4}$ Hz to $\sim 7 \times 10^{-3}$ Hz. This suggests that heightened susceptibility of sea level (but not necessarily currents) at Crescent City Harbor to tsunami is not due primarily to harbor resonances.

6. REFERENCES

Campbell, Robert (www.robertcampbellphotography.com), *Crescent City California Harbor, Aerial View*. U.S. Army Corps of Engineers, Digital Visual Library. JPEG file.

Dengler, L. A. and O. J. Magoon (2006), Reassessing Crescent City, California's tsunami risk, in *Proceedings of the 100th Anniversary Earthquake Conference*, 18-22 April, 2006, paper R1557.

Dengler, L. A. and B. Uslu (2011), Effects of Harbor Modification on Crescent City, California's Tsunami Vulnerability. *Pure and Applied Geophysics*, 168, 1175-1185.

Donn, William L. and David M. Wolf (1972), Seiche and water level fluctuations in Grindavik harbor, Iceland. *Limnology and Oceanography*, 17 (4), 639-643.

Filloux, J.H., D.S. Luther, and A.D. Chave (1991), Update on seafloor pressure and electric field observations from the north-central and northeastern Pacific: Tides, infratidal fluctuations, and barotropic flow, in *Tidal Hydrodynamics*, edited by B. B. Parker, pp. 617-639, John Wiley, New York.

Gonzalez, F. I., K. Satake, E. F. Boss and H. O. Mofjeld (1995), Edge wave and non- trapped modes of the 25 April 1992 Cape Mendocino tsunami, *Pure and Applied Geophysics*, *144*, 409–426.

Hatori, H. (1993), Distribution of tsunami energy on the circum-Pacific zone, in *Proceedings, IUGG/IOC International Tsunami Symposium*, Wakayama, Japan.

Holmes-Dean, Linda C., P. D. Bromirski, R. E. Flick, M. C. Hendershott, O. T. Magoon, and T. R. Kendall (2009), Water Levels at Crescent City Associated with the Great Chilean Earthquake of May 1960, *Scripps Institution of Oceanography Technical Report*, http://escholarship.org/uc/item/63z9j47t#, 67 pp.

Horillo, J., W. Knight and Z. Kowalik (2008), The Kuril Islands tsunami of November 2006, Part II: Impact at Crescent City by local enhancement, *J. Geophys. Res.*, *113*, C01021, doi:10.1029/2007JC004404.

Kendall, T. R., L. Dean, O. T. Magoon, L. A. Dengler, R.E. Flick, P. D. Bromirski (2008), High Resolution Analysis of the 1960 Chilean Tsunami at Crescent City, California, in *Proc., Solutions to Coastal Disasters 2008: Tsunamis*, Amer. Soc. Civil Eng., pp. 169-177, doi:10.1061/40978(313)16.

Lee J-J., Huang, Z., Kou, Z. and Xing, X. (2012), The Effect of Tide Level on the Tsunami Response of Coastal Harbors, in *Coastal Engineering Proceedings*, 1(33), doi:10.9753/ice.v33.currents.11.

Magoon, O. T. (1962), The Tsunami of May 1960 as it affected Northern California, *Conf., ASCE Hydraulics Div.*, U. CA, Davis, California, 19 pp.

Miles, J. W. (1974), Harbor Seiching, *Ann. Rev. Fluid Mech.,* 6, 17-35.

Okihiro, M., R.T. Guza, W.C. O'Reilly and McGehee (1994), Selecting Wave Gauge Sites for Monitoring Harbor Oscillations: A Case Study for Kahului Harbor, Hawaii, CERC-94-10, U. S. Army Corps of Engineers, Waterways Experiment Station.

Rabinovich, A., K. Stroker, R Thomson and E. Davis (2011), DARTs and CORE in Cascadia Basin High-resolution observations of the 2006 Sumatra tsunami in the northeast Pacific. *J. Geophys. Res.*, 38(L08607), doi:10.1029/2011GL047026.

Rayleigh, Lord (1904), On the open organ-pipe problem in two dimensions. **Phil. Mag.** (5) 1,257-279.

Roberts, J. A. and Chien, C.-W. (1964), The Effects of Bottom Topography on the Refraction of the Tsunami of 27-28 March 1964: The Crescent City Case, Meteorology Research, Inc. Report.

Wiegel, R. L. (1976), Tsunamis, in *Seismic Risk and Engineering Decisions*, edited by C. Lomnitz and E. Rosenblueth, pp. 225-286, Elsevier Scientific Publishing Company, Amsterdam.

Wilson, Basil and Torum, A. (1968), The Tsunami of the Alaskan Earthquake, 1964: Engineering Evaluations, Army Coastal Engineering Research Center, Washington, DC, 469 pp.